Topology Optimization for Loads with Multiple Points of Application

Hussein Ismail*, Matteo Bruggi**, János Lógó***

*Budapest University of Technology and Economics, Department of Structural Mechanics, Műegyetem rkp. 3, H-1111 Budapest, Hungary and Politecnico di Milano, Department of Civil and Environmental Engineering, P.zza Leonardo da Vinci, 32 20133 Milano Italy, hussein.ismail@emk.bme.hu, hussein.ismail@polimi.it

**Politecnico di Milano, Department of Civil and Environmental Engineering, P.zza Leonardo da Vinci, 32 20133 Milano Italy, matteo.bruggi@polimi.it

***Budapest University of Technology and Economics, Department of Structural Mechanics, Műegyetem rkp. 3, H-1111 Budapest, Hungary, logo.janos@emk.bme.hu

Abstract: The optimal design for loads with multiple points of application is herein investigated by using a formulation of displacement-constrained minimum volume topology optimization. For each one of the several points in which a moving force may be applied, a static load case is introduced, and a local enforcement is implemented to control the relevant displacement. Inspired by some recent contributions in stress-based topology optimization of large-scale structures, an Augmented Lagrangian approach, is adopted to handle efficiently the arising multi-constrained problem, in conjunction with mathematical programming. The results of some numerical simulations are shown to comment on optimal shapes for loads with multiple points of application, as compared to classical solutions for fixed loads.

Keywords: topology optimization; moving loads; local constraints; structural optimization

1   Introduction

Topology optimization is a design technique that allows investigating the optimal shape of structural components by distributing material within a given design domain, given a goal and a set of constraints [1] [2]. Among the others, the design performed by distribution of isotropic material is extensively adopted to investigate lightweight structures [3-5]. By selecting the density field as the unknown that governs pointwise the elastic modulus of the material, a minimization problem can be formulated adopting as objective function the work of the external loads at

equilibrium (the so-called structural compliance), while enforcing a constraint on the allowed amount of material (the available volume fraction). This is the well-known volume-constrained minimum compliance problem [6]. Since the structural compliance equals twice the strain energy stored in the design domain, under the effect of any given load, this problem is in turn equivalent to searching for the distribution of an available amount of material that minimizes the strain energy, i.e. maximizes the overall structural stiffness. Minimum compliance problems may be solved very efficiently, see the recent contribution given in [7].

The design of two-dimensional structural components is addressed in the present work as a displacement-constrained minimum volume problem, focusing on the implementation of multiple constraints and load cases. Among the others, reference is made to [8-11] for discussions and reviews on displacement constraints in topology optimization, and to [12] for an insight on the optimal design including multiple loading. A displacement-constrained minimum volume formulation is ideally conceived to investigate lightweight design at the serviceability limit state. Indeed, displacement limits are prescribed for structural elements by technical codes, whereas the amount of material needed to fulfil these constraints is an outcome of the design problem. When the controlled displacement is that at the loaded point along the direction of the applied force, the work of the external load at equilibrium equals the scalar product of the controlled displacement and the applied force. In this case, the displacement-constrained minimum volume problem is equivalent to a classical volume-constrained minimum compliance problem. As discussed in [13], the same solution (up to a scaling) is expected to arise when considering either problem. This rationale does not apply when multiple loading or distributed loads are dealt with.

Recent contributions in stress-constrained topology optimization, see in particular [14] [15], have shown that very large sets of local enforcements can be efficiently tackled by combining sequential convex programming and Augmented Lagrangian (AL) strategies, as an effective alternative to aggregation methods. Within the family of sequential programming approaches, the Method of Moving Asymptotes (MMA) [16] is widely adopted in structural optimization since it may linearize the objective function and the constraints not only in the direct variables but also in the reciprocal ones, see e.g. the discussion on topology optimization of elastic trusses in [17] and the application in [18]. In [14] an Augmented Lagrangian approach is proposed in which the original penalization term, see [19], is normalized with respect to the number of stress constraints. This approach is implemented herein to enforce a local control of the deflection when addressing loads with multiple points of application. When dynamic effects can be neglected, the case of a moving force may be handled as a set of several static load cases (describing successive positions of the load). A displacement constraint may be therefore implemented for each one of the load cases, to control the relevant displacement at the loaded node. Reference is also made to [20] [21], for examples of application of structural optimization on this topic.

While most of the methods available in topology optimization deal with volume-constrained minimum compliance optimization, the proposed approach is concerned with the application of multiple local constraints to control the displacement field. Indeed, when dealing with the design of structural components at the serviceability limit state, prescriptions on the admissible deflection must be fulfilled. A peculiarity of the proposed approach consists in the adoption of the AL strategy to handle large sets of displacement constraints. Leveraging this framework, it is possible to control the deflection at each one of the loaded points when addressing distributed loads and (static) moving loads. The former case is frequently encountered in problems of structural design, see Figure 1(left): given a geometric domain with prescribed supports, the best shape is sought to carry a distributed load while fulfilling constraint for the deflection along the edge where the load is applied. The latter case is peculiar to the conceptual design of bridges or elements supporting overhead cranes, see Figure 1(right): the desired optimal shape must carry a load with multiple points of application, with full control of the deflection caused by the load in each one of its possible positions.
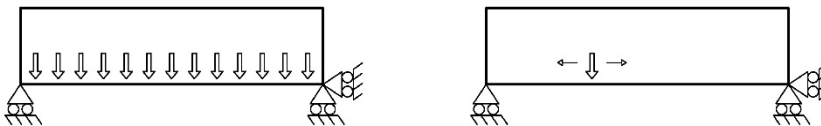

Figure 1

Design domain and boundary conditions for two problems of structural design: the case of distributed loads (left), and the case of (static) moving forces (right)

It is finally stated that, accounting for the wide variety of topology optimization methods for structural design, see in particular [1, 3, 5], alternative strategies may be successfully implemented when modelling the problem and enforcing constraints. Among the others, reference is made to the use of polygonal finite elements in topology optimization to solve the elastic problem [22], thus minimizing any mesh-related polarization in the research of optimal distributions of material when using standard four-node elements, see also [23]. It is finally remarked that the uncertainty inherent in material properties, loads, and boundary conditions of any structural design problem can be conveniently embedded in the optimization, see e.g., the reliability-based topology optimization with displacement limit state function discussed in [24]. This topic will be object of future extensions of the method.

The organization of the paper is as follows. Section 2.1 presents the displacement-constrained formulation, whereas Section 2.2 gives details on the numerical implementation, including the computation of the sensitivity information by means of the adjoint method. In Section 3 numerical applications are shown pointing out mechanical features of the achieved optimal layouts. They are focused on simple examples (rather than industrial applications), due to the main goal of preliminary assessing the proposed method through benchmark. Finally, conclusions are drawn based on the outcome of the numerical tests.

2 Problem Formulation and Implementation

When dealing with the considered multi-constrained problem of topology optimization, the finite element method is used to solve the governing equation, herein the linear elastic equilibrium. The element-wise constitutive properties of the material depend on the set of optimization unknowns through an interpolation law. A gradient-based minimization algorithm is used to iteratively update the unknowns in order to find the set that minimizes the objective function, accounting for the enforced constraints. In each step, a finite element analysis is performed to solve the elasticity problem with the current distribution of unknowns to compute updated information for the minimizer.

2.1 Problem Statement

Standard four-node displacement-based elements are used to get a discretization of a given design domain. A discrete design variable is assigned to each element. In the e-th of the n elements belonging to the mesh, $0 \leq \rho_e \leq 1$ is the so-called "density" of the material. Using the Solid Isotropic Material with Penalization (SIMP) [6][25], the constitutive matrix $\boldsymbol{C}(\rho_e)$ reads:

$$\boldsymbol{C}(\rho_e) = \rho_e^p \boldsymbol{C_0} + \boldsymbol{C_{min}} \tag{1}$$

where $\boldsymbol{C_0}$ is the plane stress constitutive matrix at full density, $\boldsymbol{C_{min}} = 10^{-9}\boldsymbol{C_0}$ stands for "void" and p is an interpolation parameter that penalizes intermediate densities, see in particular [7]. In the numerical simulations, p is increased from 3 to 9 during the optimization by means of the continuation approach used in the referenced work.

The statement of the displacement-constrained problem of minimum volume topology optimization [12] is:

$$\begin{cases} \min_{0 \leq \rho_e \leq 1} V = \sum_{e=1}^n \rho_e V_{0,e} \\ \text{subject to} \quad \left(\sum_{e=1}^n \rho_e^p \boldsymbol{K_{0,e}}\right)\boldsymbol{U}_j = \boldsymbol{F}_j, \quad \text{for } j = 1, \dots l \\ \qquad\qquad\quad u_i \leq u_{lim,i}, \qquad\qquad \text{for } i = 1, \dots m \end{cases} \tag{2}$$

In the above problem, the objective function is the volume of the structural element V. This may be computed through the sum over the contributions $\rho_e V_{0,e}$, being $V_{0,e}$ the volume of the e-th element at full density, that is for $\rho_e = 1$.

The first constraint in Eqn. (2) prescribes the static equilibrium of the structural element under multiple load cases. The global stiffness matrix is given by the element contributions accounting for the constitutive law of Eq. (1). The element stiffness matrix reads $\rho_e^p \boldsymbol{K_{0,e}}$, where $\boldsymbol{K_{0,e}}$ refers to $\rho_e = 1$. For the j-th of the l load cases, $\boldsymbol{F}_j$ is the load vector, and $\boldsymbol{U}_j$ is the relevant nodal displacement vector. Design-independent loads are dealt with in the numerical investigations that follow.

The i-th of the m displacement components to be controlled is denoted by u_i. The second constraint in Eqn. (2) enforces a prescribed limit $u_{lim,i}$. This quantity $u_{lim,i}$ stands for the maximum value that the i-th displacement component is allowed to undergo at the serviceability limit state. Assuming that u_i is an entry of $\boldsymbol{U}_j$, meaning that the i-th constraint refers to the j-th load case, one has:

$$u_i = \boldsymbol{L}_i^T \boldsymbol{U}_j \tag{3}$$

where $\boldsymbol{L}_i$ is a vector made of zeros with the exception of the entry referring to the i-th displacement degree of freedom, which takes unitary value.

2.2 Numerical Details

In this section, an insight is given on the treatment of the density field to avoid well-known numerical instabilities while achieving crisp black/white layouts, and on the gradient-based approach used to handle the arising multi-constrained problem.

2.2.1 Filtering and Projection

A linear filter [26] [27] is implemented on the element variables ρ_e to avoid the arising of checkerboard patterns and mesh dependence. The original variables ρ_e are mapped to the new set of $\tilde{\rho}_e$ as:

$$\begin{aligned}
\tilde{\rho}_e &= \frac{1}{\sum_n H_{es}} \sum_n H_{es} \rho_s \\
H_{es} &= \max(0, r_{min} - \text{dist}(e,s))
\end{aligned} \tag{4}$$

where $\text{dist}(e,s)$ is the distance between the centroid of the e-th and s-th element, and r_{min} is the filter radius, both entering the weight factor H_{es}. The filtered densities $\tilde{\rho}_e$ are subsequently mapped to the set of physical densities $\hat{\rho}_e$ to get crisp black/white solutions, see the projection proposed in [28]:

$$\hat{\rho}_e = \frac{\tanh(\beta\eta) + \tanh(\beta(\tilde{\rho}_e - \eta))}{\tanh(\beta\eta) + \tanh(\beta(1-\eta))} \tag{5}$$

with $\eta = [0,1]$ and $\beta = [1, \infty]$. In the numerical simulations, $\eta = 0.5$, whereas β is smoothly increased during the run from 2 to 16, by means of the continuation approach used in [7]. The layout of the optimal solution is given using maps of $\hat{\rho}_e$.

2.2.2 Solving Algorithm

The optimization problem in Eqn. (2) is solved via mathematical programming, using the Method of Moving Asymptotes (MMA) [16] as minimizer. Displacement constraints are treated following the Augmented Lagrangian method implemented in [14]. Constraints are gathered in a modified version of the objective function such that the problem is turned into an unconstrained minimization. At the k-th AL step, this objective function reads:

$$V = V + \frac{1}{m}\sum_{i=1}^{m}\left(a_i^{(k)}\frac{u_i}{u_{lim,i}} + \frac{1}{2}b^{(k)}\left(\frac{u_i}{u_{lim,i}}\right)^2\right) \tag{6}$$

where $a_i^{(k)}$ is the i-th entry of the vector of the Lagrangian multiplier estimators and $b^{(k)} > 0$ is a penalty factor. MMA is used to find an approximate solution of the normalized function in Eqn. (6). This solution allows updating the current values of the estimators of the Lagrangian multipliers and the penalty factor for the subsequent AL step. In the numerical simulations, the number of MMA iterations per AL step has been set to 5.

The overall process is repeated until convergence is met, i.e. the maximum difference in terms of the minimization unknowns between two subsequent steps is less than 10^{-3}.

2.2.3   Sensitivity Computation

The adjoint method is used to compute derivatives in order to provide the gradient-based minimizer with the sensitivity with respect to the design variables, see e.g. [1]. Accordingly, u_i of Eqn. (3) does not change when a zero function is added at the right hand side. Exploiting the discrete equilibrium in Eqn. (2), denoting by $K(\boldsymbol{\rho})$ the overal sriffenss matrix depending on the vector gathering the element unknowns, one may write:

$$-\lambda_i^T\big(K(\boldsymbol{\rho})U_j - F_j\big) \tag{7}$$

where λ_i is any arbitrary but fixed vector. After re-arrangement of terms, the derivative of u_i with respect to the h-th entry of $\boldsymbol{\rho}$ may be computed as:

$$\frac{\partial u_i}{\partial \rho_h} = \left(L_i^T - \lambda_i^T K(\boldsymbol{\rho})\right)\frac{\partial U_j}{\partial \rho_h} - \lambda_i^T\frac{\partial K(\boldsymbol{\rho})}{\partial \rho_h}U_j \tag{8}$$

that can be in turn written as:

$$\frac{\partial u_i}{\partial \rho_h} = -\lambda_i^T\frac{\partial K(\boldsymbol{\rho})}{\partial \rho_h}U_j \tag{9}$$

In the above expression, λ_i satisfies the adjoint equation:

$$K(\boldsymbol{\rho})\lambda_i = \left(\frac{\partial u_i}{\partial U_j}\right)^T = L_i \tag{10}$$

Eqn. (9) can be evaluated recalling that the derivative of the e-th element stiffness matrix with respect to ρ_h is equal to $p\rho_e^{p-1}\,K_{0,e}$, being $K_{0,e}$ the element stiffness matrix at full density. This sensitivity is null if $e \neq h$.

The derivatives with respect to the filtered variables $\tilde{\rho}_e$ and the physical ones $\hat{\rho}_e$ can be evaluated by applying the chain rule to Eqn. (4) and Eqn. (5), respectively. At each iteration in the process, only one matrix inverse must be computed to evaluate constraints and their sensitivities. This is because the linear systems in the first constraint of Eqn. (2) and Eqn. (11) share the same coefficient matrix $K(\boldsymbol{\rho})$.

It is also remarked that this framework is ideally conceived for a straightforward implementation within commercial finite element codes, exploding their application programming interfaces, see e.g. [29].

3   Numerical Simulations

Numerical simulations considering the optimal design under displacement constraints are presented in this section, dealing with fixed point forces, uniformly distributed loads, and forces with multiple points of application. The latter are referred to as moving point forces in the discussion that follows.

In all the examples, the controlled displacements u_i are those read at the m loaded nodes in the direction of the acting force. The limit $u_{lim,i}$ is defined either as $\alpha u_{0,i}$, i.e. α times the value found at the same point in case of full material beam $u_{0,i}$, or as $\alpha \max_m u_{0,i}$. In the former case, the goal is reproducing the stiffness provided by a full material beam, with the scaling given by α. In the latter case, the bound of the displacement is the same for all the controlled points, as conventionally done in the assessment of structures at the serviceability limit state. In the numerical simulations that follow $\alpha = 1.50$.

Rectangular domain analyzed next have height equal to L and filter radius $r_{min}=L/10$. All the layouts presented next are respectful of all the enforced local constraints. Each solution is endowed with the value of the volume fraction of the material at convergence v_f, that is the ratio of the last value of the objective function in Eqn. (2) to the volume of a full material beam.

3.1   Cantilever Beam

The first numerical investigation refers to a 3L × L cantilever beam that is fully clamped at the left side. A mesh of 300 × 100 four-node elements is used. At first, it is assumed that the specimen is acted upon by a vertical force located at the bottom right corner of the rectangular domain. According to Maxwell's principle for elements in bending having constant cross-section, this is the location of a vertical force moving along the bottom side of the rectangular domain, such that the deflection of the element is the largest one. The formulation in Eqn. (2) is implemented considering one load case ($l = 1$) and controlling the vertical component of the displacement read at the loaded point, that is the lower corner of the tip ($m = 1$). The achieved design is the truss-like structure shown in Figure 2. The volume fraction is $v_f = 0.50$. This means that only half of the material making a full material beam is needed if an increase by half in the deflection is allowed.

Figure 2

Cantilever beam: optimal design considering a force applied at the tip (v_f = 0.50)

A second investigation is performed considering a uniformly distributed load acting all over the lower side of the rectangular domain. A set of constraints is enforced in the formulation of Eqn. (2) to control the vertical displacement at each one of the loaded nodes within the same load case ($l = 1$, $m = 300$). The optimal layouts that are found by enforcing the same u_{lim} throughout the span ($\alpha \max_m u_{0,i}$) and by implementing the varying u_{lim} ($\alpha u_{0,i}$), are shown in the left and right picture of Figure 3, respectively.

Figure 3

Cantilever beam: optimal design considering a uniformly distributed load, for the same u_{lim} all over the span (left, v_f = 0.40), and varying u_{lim} to approximate the deflection of a full beam (right, v_f = 0.50)

The relevant deformed shapes are sketched in Figure 4, along with a horizontal line representing the quantity $\alpha \max_m u_{0,i}$. In the latter case, the design is heavier than in the former (v_f = 0.50 vs. 0.40) due to the stricter displacement constraints. Indeed, almost one half of the bottom side of the domain lies along the line representing the quantity $\alpha \max_m u_{0,i}$ in the former case, whereas in the latter such a deflection is allowed at the tip only.

Figure 4

Cantilever beam: deformed shapes of the layouts achieved considering a uniformly distributed load: same u_{lim} all over the span (left), and varying u_{lim} to approximate the deflection of a full beam (right)

Two additional simulations are set to investigate the difference between displacement-constrained minimum volume optimization and volume-constrained minimum compliance design. Minimum compliance layouts are found using as

input the volume fractions found in output for the minimum volume layouts of Figure 3. The optimal layouts (in their deformed configuration) for $v_f = 0.40$ and $v_f = 0.50$ are represented in the left and right picture of Figure 5, respectively. In both pictures, the horizontal line representing the quantity $\alpha \max_m u_{0,i}$ already used in Figure 4 is reported to check the deformability. The achieved minimum compliance layouts have some similarity with the minimum volume design approximating the deflection of a full material beam, see Figure 3 (right). However, as expected, neither of them is stiff as the solutions found by enforcing a local control of the displacement field.

Figure 5
Cantilever beam: deformed shapes of the minimum compliance layouts achieved considering a uniformly distributed load and prescribing: $v_f = 0.40$ (left), and $v_f = 0.50$ (right)

Finally, the optimal design in case of a point force moving along the lower side of the geometrical domain of the cantilever is considered. This may be simply implemented in Eqn. (2) by defining a load case for each one of the nodes belong to the load path of the point force ($l = 300$), and by controlling the relevant displacement at the loaded node ($m = 300$). Along the lines of the simulations performed in case of uniformly distributed load, two optimization strategies have been tested. The picture on the left in Figure 6, is the layout achieved by enforcing the same displacement limit all over the load cases ($\alpha \max_m u_{0,i}$). The optimal design has the same volume fraction of the optimal design found in the case of a specimen loaded by a vertical force at the tip. However, it has less and thicker members than the layout in Figure 2. Dealing with the moving force, a subsequent optimization is performed using the varying u_{lim} that is aimed at reproducing the deflection of a full material beam ($\alpha u_{0,i}$). A much heavier design arises in this case to fulfil the stricter deflection constraints, see the picture on the right in Figure 6.

Figure 6
Cantilever beam: optimal design considering a moving vertical force, for the same u_{lim} throughout the span (left, $v_f = 0.50$), and varying u_{lim} to approximate the deflection of a full beam (right, $v_f = 0.58$)

3.2 Single Span Beams

In this section the displacement-constrained minimum volume design is investigated dealing with single span beams occupying a rectangular domain with size $6L \times L$. A mesh of 600×100 four-node elements are used. Forces are applied at the lower side of the rectangular domain.

At first, the case of simply supported beam is considered. Figure 7 gathers pictures representing the optimal layouts found when considering a force applied at midspan (top), a uniformly distributed load (center), and a moving vertical force (bottom). The last two layouts have been found by enforcing the same displacement limit all over the loaded points ($\alpha \max_{m} u_{0,i}$). The optimal design achieved in case of uniformly distributed load takes full advantage of the symmetry of the load and of the low value of the shear force around midspan. The solution found for the moving force is a more branched variation of that found considering a force applied at midspan. Indeed, this is the location of the point force for which the deflection is the largest in a beam with uniform cross section. The achieved design costs a very minor increase in terms of volume fraction ($v_f = 0.52$ vs. 0.50).

Then, the case of a two hinged beam is analyzed, considering the same loads and optimization problems already implemented for the simply supported beam. The achieved results are given in Figure 8. The optimal layout found for the uniformly distributed load is an efficient arch-like structure with inclined ties, a widely implemented solution in bridge design. In the solution found considering a force applied at midspan, the point load hangs from a central stiff region that is supported by two inclined struts. This layout cannot accommodate effectively forces with different point of applications. Indeed, the optimal solution found for the moving point force is a much heavier structure: the arch already exploited in the design for the uniformly distributed load is here endowed with a strut-and-tie substructure that supports the point force all over its path.

Figure 7

Simply supported beam: optimal design considering a force applied at midspan (top, $v_f = 0.50$), a uniformly distributed load (center, $v_f = 0.37$), and a moving vertical force (bottom, $v_f = 0.52$)
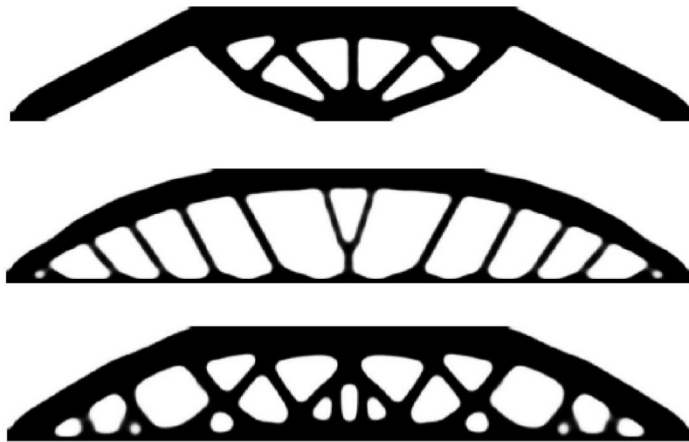
Figure 8

Hinged beam: optimal design considering a force applied at midspan (top, $v_f = 0.42$), a uniformly distributed load (center, $v_f = 0.36$), and a moving vertical force (bottom, $v_f = 0.53$)

3.3   Two-Span Beam

A two-span beam is considered adopting the same mesh used in the previous example. An additional support is added in the middle of the lower side. At first the optimal design is dealt with considering a uniformly distributed load applied at the lower edge all over the two spans ($l = 1$ and $m = 598$). The same displacement limit ($\alpha \max_m u_{0,i}$) is enforced at all the loaded points. The optimal design is represented in the top picture of Figure 9. The arm between the upper and the lower chord of the structure is in good agreement with the diagram of the bending moment of a two-span beam made of full material. To maximize the deflection, an alternative load scenario could be conveniently considered. The optimal design shown in the bottom picture of Figure 9 concerns the implementation of two load cases. The uniformly distributed load acts in one span at a time, i.e. $l = 2$ and $m = 598$, with half of the constraints referring to the points loaded in the left span (first load case) and half to the points loaded in the right span (second load case). In each of the two spans the design is quite similar to that found for the simply supported beam, see Figure 7 (center).

The last set of investigations refers to a moving point force whose path is the lower side of the rectangular domain. This is implemented in Eqn. (2) by defining a load case for each one of the nodes belonging to the path followed by the point force ($l = 598$) and by controlling the relevant displacement at the loaded node ($m = 598$). As done in Section 3.1, two optimization strategies have been tested.
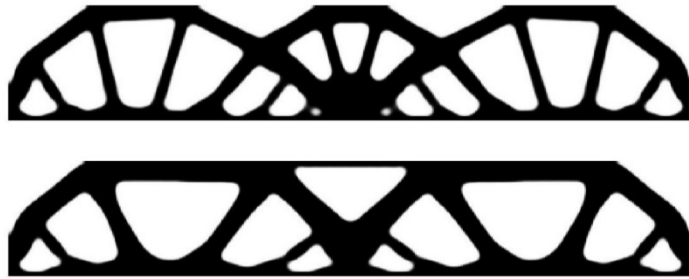
Figure 9

Two-span beam: optimal design considering a uniformly distributed load acting on both spans
simultaneously (top, $v_f = 0.46$), and acting in one span at a time (bottom, $v_f = 0.50$)

In Figure 10 the optimal layout achieved by enforcing the same displacement limit
all over the load cases ($\alpha \max_{m} u_{0,i}$) is represented. In Figure 11 the optimal design
achieved by enforcing the varying u_{lim} that is aimed at reproducing the deflection of
a full material beam ($\alpha u_{0,i}$) is given. In both figures a map of the vertical
displacements computed at the varying loaded point is provided, along with a plot
of the fixed/ varying u_{lim}. Although the optimal layouts are quite similar in terms of
topology and volume fraction ($v_f = 0.62$ vs 0.65), the relevant displacement plots
are quite different. While most of the deck undergoes the maximum allowed
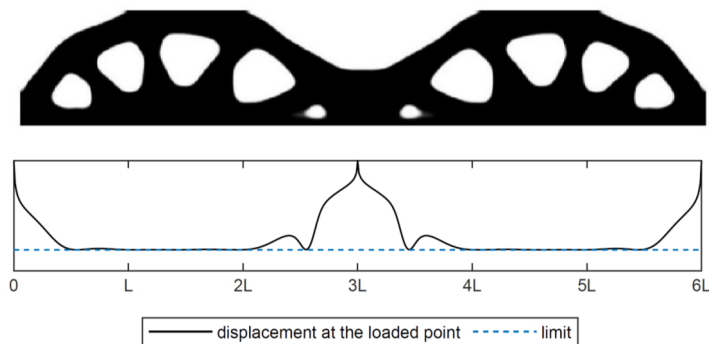displacement in the former case, a smoother variation is found, as expected, in the
latter.

Figure 10

Two-span beam: design considering a moving vertical force and the same u_{lim} throughout the spans (v_f
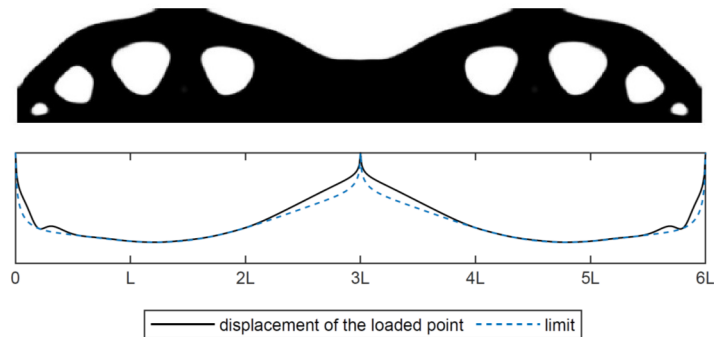= 0.62): optimal layout and displacement computed at the varying loaded point

Figure 11

Two-span beam: design considering a moving vertical force and a varying u_{lim} aimed at approximating the deflection of a full beam ($v_f = 0.65$): optimal layout and displacement computed at the varying loaded point

Conclusions

A formulation of topology optimization, by distribution of isotropic material, has been proposed, searching for structures of minimum volume subjected to multiple displacement constraints. The same problem can deal with fixed point or distributed loads and forces with multiple points of application. Indeed, for each one of the several points, in which a moving force may be applied, a local enforcement may be used to control the relevant displacement.

Following recent contributions addressing stress-based topology optimization of large-scale structures, a modified Augmented Lagrangian approach has been implemented, in conjunction with sequential convex programming, to handle the arising multi-constrained problem, in an efficient way.

Numerical simulations have been shown to elaborate on optimal design with multiple displacement constraints. Two strategies have been tested to formulate enforcements regarding the deflection: as conventionally done at the serviceability limit state, the same upper bound of the displacement can be used for all the controlled points. Alternatively, a varying limit may be used to mimic the stiffness provided by a full material beam. Optimal solutions for moving loads have been compared to classical solutions for fixed loads, both point forces and distributed loads. In a few examples, the optimal topology for moving loads was found to be a slightly heavier variation of the topology obtained for a single force applied where the maximum deflection was expected (see results concerning the cantilever beam and the simply supported beam). However, alternative layouts may arise to provide the required support along the entire load path (see results on the two hinged beam). It is also remarked, that the strategy adopted to enforce deflection constraints remarkably affects, as expected, the displacement read under the moving force (see results on the two-span beam).

The proposed design tool can be conveniently used to sketch preliminary solutions for any load conditions and restraint configurations. It is finally remarked that the considered multi-constrained formulation could be effectively augmented with other types of enforcements, such as buckling constraints and stress constraints, with the main aim of designing effective structural components [30]. The ongoing research is devoted to the extension of the proposed approach to multiscale design, moving from a deterministic framework, to a probabilistic one, implementing the methods proposed in [31-33].

Acknowledgement

References

[1]   M. P. Bendsøe, O. Sigmund, Topology Optimization: Theory, Methods and Applications. Berlin: Springer, 2003

[2]   T. Lewiński, T. Sokół, C. Graczykowski, Michell structures. Berlin: Springer, 2018

[3]   O. Sigmund, K. Maute, "Topology optimization approaches: A comparative review", *Struct. Multidiscip. Opt.*, Vol. 48(6), pp. 1031-1055, 2013

[4]   W. Zhang, J. Zhu, T. Gao, Topology Optimization in Engineering Structure Design. London: Elsevier; 2016

[5]   J. Lógó, H. Ismail, "Milestones in the 150-year history of topology optimization: A review", *Comput. Assist. Methods Eng. Sci.*, Vol. 27(2-3), pp. 97-132, 2020

[6]   M. P. Bendsøe, N. Kikuchi, "Generating optimal topologies in structural design using a homogenization method", *Comput. Methods Appl. Mech. Eng.*, Vol. 71(2), pp. 197-224, 1988

[7]   F. Ferrari, O. Sigmund, "A new generation 99 line Matlab code for compliance topology optimization and its extension to 3D", *Struct. Multidiscip. Optim.*, Vol. 62, pp. 2211-2228, 2020

[8]   M. Kočvara, "Topology optimization with displacement constraints: A bilevel programming approach", *Struct. Opt.*, Vol. 14(4), pp. 256-263, 1997

[9]   L. Yin, W. Yang, "Optimality criteria method for topology optimization under multiple constraints", *Comput. Struct.*, Vol. 79(20-21), pp. 1839-1850, 2001

[10]   J. H. Rong, X. H. Liu, J. J. Yi, J. H. Yi, "An efficient structural topological optimization method for continuum structures with multiple displacement constraints", *Finite Elem. Anal. Des.*, Vol. 47(8), pp. 913-921, 2011

[11]   A. Csébfalvi, "Volume minimization with displacement constraints in topology optimization of continuum structures", *Int. J. Optim.*, Vol. 6(3), pp. 447-453, 2016

[12]   J. Lógó, B. Balogh, E. Pintér, "Topology optimization considering multiple loading", *Comput. Struct.*, Vol. 207, pp. 233-244, 2018

[13]   W. Achtziger, "Topology Optimization of Discrete Structures", in Topology Optimization in Structural Mechanics, Rozvany G.I.N. Ed., International Centre for Mechanical Sciences (Courses and Lectures), Vol. 374, Vienna: Springer, 1997

[14]   O. Giraldo-Londoño, G. H. Paulino, "PolyStress: A matlab implementation for local stress-constrained topology optimization using the augmented lagrangian method", *Struct. Multidiscip. Optim.*, Vol. 63(4), pp. 2065-2097, 2021

[15]   G. A. da Silva, N. Aage, A. T. Beck, O. Sigmund, "Three-dimensional manufacturing tolerant topology optimization with hundreds of millions of local stress constraints", *Int. J. Numer. Methods Eng.*, Vol. 122(2), pp. 548-578, 2021

[16]   K. Svanberg, "Method of moving asymptotes - A new method for structural optimization", *Int. J. Numer. Methods Eng.*, Vol. 24(2), pp. 359-373, 1987

[17]   P. W. Christensen, A. Klarbring, An introduction to structural optimization. Berlin: Springer, 2008

[18]   M. Bruggi, "A constrained force density method for the funicular analysis and design of arches, domes and vaults", *Int. J. Solids Struct.*, Vol. 193-194, pp. 251-269, 2020

[19]   D. P. Bertsekas, Nonlinear programming, 2nd edn. Nashua: Athena Scientific, 1999

[20]   R. H. Zuberi, Z. Zhengxing, L. Kai, L. Wen, "Topological optimization of constant beam section under moving load condition", *2010 International Conference on Mechanic Automation and Control Engineering*, pp. 354-359, 2010

[21]   S. Zhang, J. Yin, Y. Liu, F. Ma, Z. Sha, D. Yang, "Structural topology optimization of brake disc using the equivalent moving load method", *J. Eng. Tech. Sci.*, Vol. 51(6), pp. 791-804, 2019

[22]   C. Talischi, G. H. Paulino, A. Pereira, I. F. M. Menezes, "Polygonal finite elements for topology optimization: A unifying paradigm", *Int. J. Numer. Methods Eng.*, Vol. 82(6), pp. 671-698, 2010

[23]   K. Chandrasekhar, V. Bhikshma, S. Mohi, "On the Six Node Hexagon Elements for Continuum Topology Optimization of Plates Carrying in Plane Loading and Shell Structures Carrying out of Plane Loading", *J. Appl. Comput. Mech.*, Vol. 6(3), pp. 617-639, 2020

[24] R. Amaral, J. Borges, H. Gomes, "Proportional Topology Optimization under Reliability-based Constraints", *J. Appl. Comput. Mech.*, Vol. 8(1), pp. 319-330, 2022

[25] M. Zhou, G. I. N. Rozvany, "The COC algorithm, Part II: Topological, geometrical and generalized shape optimization", *Comput. Methods. Appl. Mech. Eng.*, Vol. 89(1-3), pp. 309-336, 1991

[26] T. Borrvall, J. Petersson, "Topology optimization using regularized intermediate density control", *Comput. Methods. Appl. Mech. Eng.*, Vol. 190(37-38), pp. 4911-4928, 2001

[27] B. Bourdin, "Filters in topology optimization", *Int. J. Numer. Methods Eng.*, Vol. 50(9), pp. 2143 2158, 2001

[28] F. Wang, B. Lazarov, O. Sigmund, "On projection methods, convergence and robust formulations in topology optimization", *Struct. Multidiscip. Optim.*, Vol. 43(6), pp. 767-784, 2011

[29] D. Briccola, M. Bruggi, "Analysis of 3D linear elastic masonry-like structures through the API of a finite element software", *Adv. Eng. Softw.*, Vol. 133, pp. 60-75, 2019

[30] B. Blachowski, P. Tauzowski, J. Lógó, "Yield limited optimal topology design of elastoplastic structures", *Struct. Mutltidiscip. Opt.*, Vol. 61(5), pp. 1953-1976, 2020

[31] M. Bruggi, A. Taliercio, "Hierarchical infills for additive manufacturing through a multiscale approach", *J. Optim. Theory Appl.*, Vol. 187(3), pp. 654-682, 2020

[32] B. Balogh, M. Bruggi, J. Lógó, "Optimal design accounting for uncertainty in loading amplitudes: A numerical investigation", *Mech. Based Des. Struct.* Mach., Vol. 46(5), pp. 552-566, 2018

[33] P. Tauzowski, B. Blachowski, J. Lógó, "Topology optimization of elasto-plastic structures under reliability constraints: A first order approach", *Comput. Struct.*, Vol(243), n. 106406, 2021